Estimations of soil metal accumulation or leaching potentials under climate change scenarios: the Example of copper on a European scale

Laura SERENI[1,2], Julie-Maï PARIS[3], Isabelle LAMY[1], Bertrand GUENET[3]

[1]Université Paris-Saclay, INRAE, AgroParisTech, UMR EcoSys, 91120 Palaiseau, France

[2]Present address: Univ. Grenoble Alpes, CNRS, INRAE, IRD, Grenoble INP, IGE, Grenoble, France

[3]Laboratoire de Géologie ENS, PSL Research University, CNRS, UMR 8538, IPSL, Paris, France

*_Correspondence to_ Laura Sereni (laurasereni@yahoo.fr)

Abstract:

Contaminants inputs to soil are highly dependent on anthropogenic activities while contaminant retention, mobility and availability are highly dependent on soil properties. The knowledge of partitioning between soil solid and solution phases is necessary to estimate whether deposited amounts of contaminants will rather be transported with runoff or accumulated. Besides,, runoff is expected to change during the next century due to changes in climate and in rainfall patterns. In this study, we aimed at estimating at the European scale the areas with a potential risk due to contaminant leaching (LP). We also defined in the same way the surface areas where limited Cu leaching occurred, leading to potential accumulation (AP) areas. We focused on copper (Cu) widely used in agriculture under mineral form or associated to organic fertilizers, resulting in high spatial variations in deposited and incorporated amounts in soils as well than in European policies of application. We developed a method using both Cu partition coefficients (K_f) between total and dissolved Cu forms, and runoff simulation results for historical and future climates. The calculation of K_f with pedo-transfer functions allowed us to avoid any uncertainties due to past management or future depositions that may affect total Cu concentrations. Areas with high potential risk of leaching or of accumulation were estimated over the 21st century by comparing K_f and runoff to their respective European median. Thus, at three distinct times, we considered a grid cell at risk of LP if its K_f was low compared to the European median and its runoff was high compared to the European median of the time. Similarly, a grid cell was considered at risk of AP if its K_f was high and its runoff was low compared to their respective European median of the time. To deal with uncertainties in climate change scenarios and the associated model prediction, we performed our study with two representative atmospheric greenhouse gases concentration pathways (RCP), defined with climate change associated to a large set of socio-economic scenarios found in the literature. We used two land surface models (ORCHIDEE and LPJmL, given soil hydrologic properties) and two global circulation models (ESM2m and CM5a, given rainfall forecast). Our results show that, for historical scenario 6.4 ± 0.1 % (median, median deviation) and 6.7 ± 1.1 % of the grid cells of the European land surfaces are with LP and AP respectively. Interestingly, we simulate a constant surface area with by LP and AP, around 13% of the grid cells, consistent with an increase in AP and a decrease in LP. Despite large variations in LP and AP extents depending on the land surface model used for estimations, the two trends were more pronounced with RCP 6.0 than with RCP 2.6, highlighting the global risk of combined

climate change and contamination and the need for more local and seasonal assessment. Results are discussed to highlight the points requiring improvement to refine predictions.

Keywords: regional modeling, transfer functions, ISIMIP, LUCAS Topsoil data, mapping risk

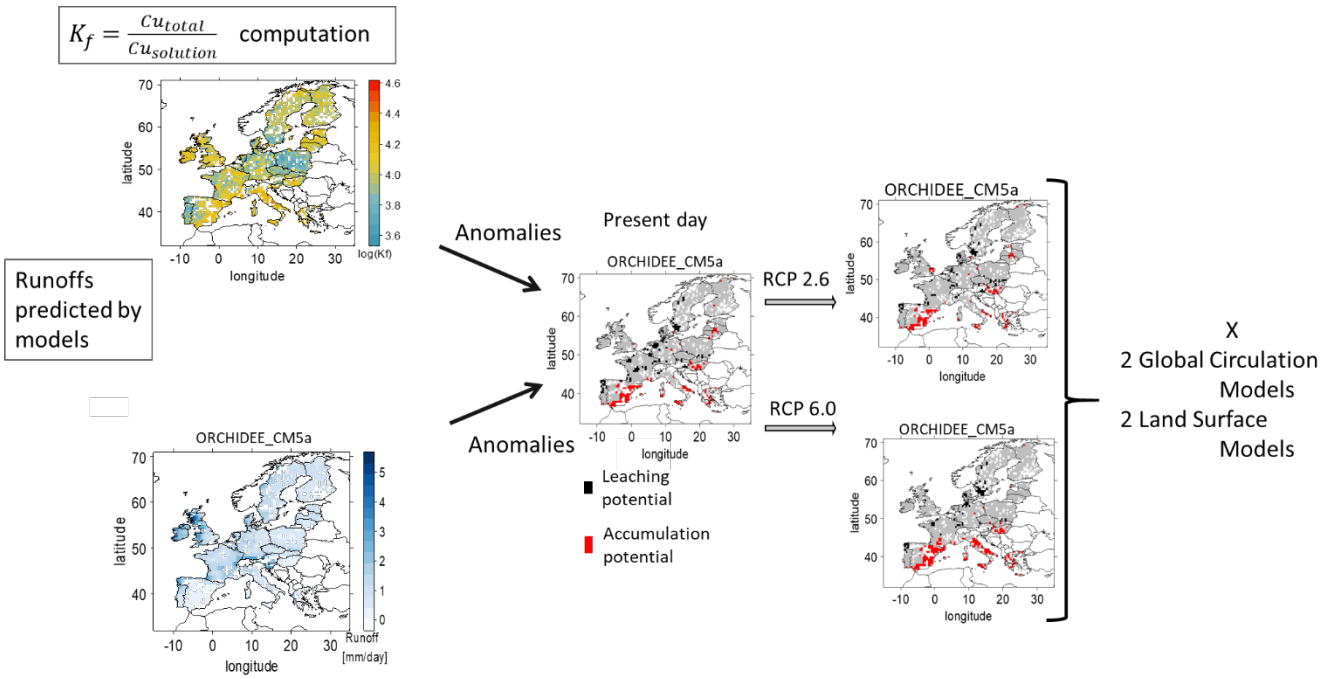

1. Introduction

At a large spatial scale, trace element contents in soils are highly variable in relation with the trace element contents of the soil parental rocks and with local anthropogenic inputs of various origins (Flemming and Trevors, 1989; Salminen and Gregorauskiene, 2000; Noll, 2003). Some trace elements like copper (Cu) or zinc are required for several biological mechanisms, but when highly concentrated they may have toxic effects on soil organisms (Giller et al., 1998). In particular, Cu is widely used as a fungicide, especially against downy mildew in vineyard parcels(Komárek et al., 2010), but also in industrial processes. Besides, Cu application to soils are numerous, in the mineral form or within the organic fertilizers applied, leading to a global European limit of application. At the European scale, a gradient of soil Cu concentrations can be find from typical baseline values between 5 $mgCu.kg^{-1}$ to 20 $mgCu.kg^{-1}$ (Salminen and Gregorauskiene, 2000), to values larger than 100 $mgCu.kg^{-1}$, common in cultivated soils and especially in vineyards parcels (Ballabio et al., 2018). It is commonly accepted to conceptually partition the total soil Cu content into different pools of Cu forms in close equilibrium. Briefly, three pools can be defined: a so-called 'inert' pool corresponding to Cu included into minerals, a so-called 'labile' pool corresponding to Cu sorbed to soil constituents but that can be mobilized according to environmental conditions, and a smallest 'mobile' pool corresponding to Cu in soil solution that may be readily available for living organisms but also for transport within soil horizons (West and Coombs, 1981; Rooney et al., 2006; Broos et al., 2007). Schematically, these pools are governed by processes like exchange, complexation or sorption. Also, local soil characteristics such as organic matter, pH or cationic exchange capacity can affect the proportion of Cu in these different pools (Vidal et al., 2009). Any modifications in soil properties or soil solution composition may thus affect Cu equilibrium between sorbed and solution phases. The pool of Cu in the solution phase can be assimilated to a potential pool of Cu leaching. Conversely, Cu bound to the solid phases can be assimilated to a potential pool of Cu accumulation in soil. Depending on the main process involved, for a given amount of Cu deposited on soil, the proportions of leached and accumulated Cu can vary from place to place and with time. However, studies simulating whether the soil will rather leach or accumulate a contaminant are scarce especially at a large spatial scale. Knowing and predicting this leaching or retention, however, could allow to highlight contaminated areas with a potential to leach, disperse or accumulate contaminants, and therefore help for long term environmental management.

Concurrently, climate change due to anthropogenic activities is expected to impact rainfall patterns in the forthcomingdecades, leading to changes in the frequency and intensity of weather events at regional and local levels (Christensen and Christensen, 2003). For instance, an increase in rain- and snow-fall events in winter in Northern Europe but a decrease in summer in the Mediterranean region are projected, which extends to northward regions (Douville et al., 2021) with extent of rain- and snow-fall alterations depending on climate change. Thus, climate change will alter the soil waterflows throughout the century (Mimikou et al., 2000). For instance, increase in rainfall intensity and in water accumulation in the soil surface due to limited water infiltration may induce large runoff (Chu et al., 2019). Changes in runoff will also change fluxes of elements or of particulates in the soil solution as it has been shown for Cu (Babcsányi et al., 2016). However, predicting how these runoff changes will relate to elemental contaminant fluxes in the coming decades remain difficult..

In this framework, our aim was twofold: i) estimate the areas the most likely to lose soil Cu within soil solution and waterflows, thereafter named leaching potential areas [LP], for the historical period (2001-2005) and ii) predict their changes according to

different climate change scenarios. Additionally, we aimed to estimate the areas the most likely to accumulate Cu, thereafter named accumulation potential areas [AP]. We hypothesized that the processes of Cu accumulation or leaching can be described by the combined effects of local runoff amounts and of local soil properties controlling the partition of total Cu in sorbed and solution species. Due to the lack of information about the future Cu deposition whatever its form, we developed a method using the partition coefficient (K_f) at the equilibrium between solid and solution phases to determine areas with high or low potential of leaching whatever total Cu concentration. Regarding the lack of data about future deposited amounts at large scale, using K_f was necessary to estimate the Cu mobility potential. The LP or AP areas were thus estimated through the combined use of K_f, calculated with the help of pedo-transfer functions, and the use of soil runoff amounts extracted from earth system simulations. With the use of K_f we avoided the uncertainties due to past land management and previous Cu deposition and focused on risks arising from future deposition. To do so, we first reviewed the empirical equations estimating Cu's K_f based on soil properties to highlight generic soil properties governing this partition. From this review, we extracted the best compromise K_f equation to estimate partitioning at the regional scale, which ensures more accurate Kf calculation based on pedo-geochemical data typically recorded in soil surveys, thus mainly available. This allowed us to estimate Cu's K_f values to be used at the European scale based on pedo-geochemical soil surveys without the knowledge of soil Cu total content. We then focused on the current state of the climate and its projected changes over the 21st century, based on two climate change scenarios. The rainfall predictions were analyzed at a 0.5° resolution, which is a common scale for land surface models allowing a multi-comparison to capture the variability in soil properties and rainfall regime. To capture the difficulties in runoff prediction and to disentangle the uncertainties between rainfall prediction and runoff calculations of land surface models, we used a set of simulations provided by the Inter-Sectoral Impact Model Intercomparison Project (ISIMIP). These simulations used different land surface models driven by different climate forcings computed by different climate models. For each scenario and each couple of land surface model and climate forcing we estimated the LP or AP of each grid cells by comparison between the local values of K_f and of runoff to the respective calculated European median that is less affected by extreme values than the arithmetic mean.

2. Materials and methods

2.1. Equations to estimate copper K_f

The rigorous definition of K_f is based on the concentration ratio of sorbed vs solution species (here Cu) at the equilibrium. Yet, for practical reasons of measurement and applicability, K_f is conventionally derived from total Cu and not from sorbed Cu (Degryse et al., 2009). A general form of the Cu partition coefficient between soil and solution – K_f – can be used to describe Cu concentrations in the sorbed and solution phases, defined as Eq. (1):

$$K_f = \frac{Cu_{total}}{Cu_{solution}{}^{n}} \quad (1)$$

Where Cu_{total} is the total Cu content of soil in $mg.kg^{-1}$, $Cu_{solution}$ is the Cu content of soil solution in $mg.L^{-1}$ and *n* stands for the variation in binding strength with metal loading (Groenenberg et al., 2010). A low K_f reflects a high proportion of Cu in solution for a given total Cu content of the soil. K_f can vary as a function of different soil parameters (Degryse et al., 2009;

Elzinga et al., 1999) and can also be estimated using Eq. (2):

$$(K_f) = a_0 + \sum_i \quad a_i log_{10}(X_i) \quad (2)$$

with X_i the different soil parameters and a_i the corresponding associated coefficient to the parameter.

Numerous studies in the literature have attempted the determination of the value of K_f. using the Eq. (2) based on statistical relationships between soil pedo-geochemical parameters, Cu in solution and total Cu measurements. The soil pedo-geochemical parameter X_i and its associated coefficient a_i can differ depending on the study and the data set used for the estimation. For the purposes of this study, K_f is estimated at the European Union level, so the formula chosen strikes the best balance between the accuracy of the relationship and its applicability on a wide scale. Thus, the equation must:

i) Include only parameters that are measured in large soil surveys

ii) Have been fitted on a large range of each soil parameter

iii) Focus on in situ long-term contamination and not on laboratory experiments.

On December 2020 we first ran a bibliographic research on WOS looking for "Cu AND availab*AND soil AND TOPIC function". We then completed this search by examining the references cited in the articles found. We collected the available relationships for estimating K_f on the basis of soil pedo-geochemical characteristics and/or total Cu. We selected only relationships that were based on commonly collected soil pedo-geochemical characteristics, such as soil organic matter (OM) or soil organic carbon (OC), dissolved organic carbon (DOC), cationic exchange capacity (CEC), clay percentage and pH that are the most frequently reported values from large scale soil survey.

2.2 Soil data

This study used European data on various soil parameters, in particular pH and organic carbon (OC), obtained from the Joint Research Centre's (JRC) LUCAS topsoil data. The data set is limited only to the territories of European Union Member States. The aforementioned data set provides information on pH (Panagos et al., 2022; Ballabio et al., 2016; ESDAC - European Commission, 2024; Panagos et al., 2012) and OC contents (Panagos et al., 2022; de Brogniez et al., 2015; ESDAC - European Commission, 2024; Panagos et al., 2012)). The data has been re-gridded with cdo commands (Schulzweida, 2019) to a spatial resolution of 0.5° (equivalent to approximately 50 km). This was done to match the resolution of the land surface models that were used to estimate the runoff. The resulting runoff data is presented in section 2.3.

2.3. Runoff data from land surface models

Runoff is computed in land models from incoming precipitations, calculated evapotranspiration, and soil hydrologic capacities. To estimate changes in soil runoff during the 21st century and to reduce uncertainties, we used two typical land-surface schemes models (LSM) – namely ORCHIDEE (Krinner et al., 2005) and LPJmL (Sitch et al., 2003)– and two global circulation models (GCM) providing climate projections – namely IPSL-CM5a (Dufresne et al., 2013) and GDFL-ESM2m (Dunne et al., 2012) – further named CM5a and ESM2m respectively. Our study exploited simulations conducted as part of the Inter-Sectoral Impact Model Intercomparison Project Phase 2b (ISIMIP2b), which supplied simulations of land surface models driven by binding scenarios from 1861 to 2099 (Frieler et al., 2017). Further details of the protocol used can be found at ISIMIP2b (The Inter-Sectoral Impact Model Intercomparison Project, 2021). The ISIMIP2b utilizes harmonized climate forcings derived from

gridded, daily bias-adjusted climate data of various CMIP5 (5th coupled model intercomparison project) global circulation models (GCMs) (Frieler et al., 2017; Lange, 2016) as well as with the use of global annual atmospheric CO_2 concentration, and harmonized annual land use maps (Goldewijk et al., 2017). The application of bias-corrected climate data ensures that the climate used by the land surface models is consistent with observations over the last 40 years of the historical period. We compared the historical data calculated by the different models with three five-year periods distributed over the 21st century: 2001-2005, called historical scenario, 2051-2055 and 2091-2095. In order to simulate 2051-2055 and 2091-2095 periods, we used two century-scale scenarios called Representative Concentration Pathway (RCP). These scenarios have been defined by the Intergovernmental Panel on Climate Change (IPCC) (van Vuuren et al., 2011) and correspond to common socio-economic pathways followed by the world's population. Here, we focused on RCP 2.6, which represents an active reduction of greenhouse gas emissions to comply with the Paris Agreement, and RCP 6.0, which represents more or less *business as usual*. RCP 2.6 is predicted to produce a radiation forcing of 2.6 $W.m^{-2}$, whereas RCP 6.0 would result in a radiation forcing of 6 $W.m^{-2}$.

For each combination of LSMs (LPJmL or ORCHIDEE) and GCMs (CM5a or ESM2m), we calculated the mean over 5 years at 3 period evenly space: 2001 - 2005, 2051 - 2055 and 2091 - 2095 of the 21st century. The cross scheme of two land surface models and two GCMs enabled us to establish whether estimations of runoff are influenced more by rainfall projection provided by the GCMs or the representation of soil hydrologic characteristics provided by the LSMs. When predictions are driven by soil hydrologic properties, highest differences in runoff predictions are expected between couple of model with the same LSM but different GCM (e.g. for instance LPJmL_CM5a is closest to LPJmL_ESM2m than to ORCHIDEE_CM5a) Contrarily, when predictions will be driven by rainfall projections, highest differences in runoff predictions are expected between couple of model with the same GCM but different LSM (e.g. for instance LPJmL_CM5a is closest to ORCHIDEE_CM5a than to LPJml_ESM2m)

2.4. Assessement of AP and LP areas

AP or LP areas were assessed by comparing the K_f and runoff values of each grid cell with its corresponding spatial median. Median runoff was computed for the whole of Europe for each five-year average period studied per model. LP areas were characterized by low K_f and high runoff, while AP areas were characterized by the opposite (see Eq. (3a) and (3b)). We identified grid cells with unusually high or low values, later referred as anomalies as grid cells above or below a 1 MAD deviation. MAD was computed as $median(|x_i| - median(x))$, x being successively runoff and K_f for the © grid cells where K_f can be estimated (see Eq. (3a) and (3b)).

For each combination of LSM (ORCHIDEE or LPJmL) x GCM (CM5a or ESM2m) and each time period (t=2001-2005; 2051-2055 or 2019-2095) with the two climate change scenarios (RCP 2.6 or RCP 6.0) applied for the periods 2051-2055 and 2091-2095, we have defined LP and AP areas as follows:

- Areas with soils exhibiting high potentiality of Cu leaching (LP areas) under 1 MAD threshold (named LP) for a 5 years mean time period *t* were defined as areas where grid cells*i* have:

$$\{K_f(i) < Median\left(European\ K_f\right) - 1\ MAD\ \left(European\ K_f\right)\ Runoff(t,i) > Median\ (European\ runoff\ (t) + 1\ MAD\ (European\ Runoff(t))\ \ (3a)$$

- Areas with soils exhibiting low potentiality of leaching corresponding to soils of high Cu accumulation potentiality (AP areas)

183 under 1 MAD threshold (named AP) for a 5 years mean time period *t* were defined as areas where grid cells *i* have:

184 $$\{K_f(i) > Median\left(European\ K_f\right) + 1\ MAD\ \left(European\ K_f\right)\ Runoff(t,i) < Median\ (European\ runoff\ (t) -$$

185 $$1\ MAD\ (European\ Runoff(t))\ \ (3b)$$

186

187 The benefit of this approach is that anomalies identification is not affected by the set of coefficients chosen to compute K_f,
188 and it removes the absolute nature of the values, but it focus on the deviation to median..

189 We choose to calculate the MAD to each time period to emphasized the spatial variability. Anomalies identification could also
190 be done using the historical runoff as a reference and looking at its change with time. However, when considering the actual
191 rainfall regime as a reference, we consider that the current environmental risk well considers the spatial risk variability.

192 In the next sections the results of temporal trends are presented using median per model and mean over the 4 models.

193 We used R 4.1.2 (R Core Team, 2021) to compute anomalies and perform the figures.
194

195 3. Results

196 3.1. K_f estimations at the European scale

197

198 The empirical equations extracted from our literature review to estimate K_f are given in Table 1. We collected 15 equations
199 allowing us to calculate K_f as the coefficient of partition between total Cu and Cu in solution. Among these equations, pH was
200 found the more decisive factor in K_f estimation (8/15 relationships). Indeed, K_f is positively correlated to pH so that the more
201 alkaline the soil is, the highest the ratio total Cu/Cu in solution is. Soil organic matter (OM) or OC is less often a parameter in
202 the K_f equations (4/15 relationships) but, when present, partial slope for OM/OC is higher than that for pH which means that
203 a small variation in soil OM content affect more Cu partitioning than a small variation in pH. Three of the 4 papers concerned
204 found a positive relationship between OM and K_f while (Mondaca et al., 2015) found a negative partial slope for soil OM or
205 dissolved OC (Table 1, Eq. (12d)). However, this Eq. (12d) was fitted on arid soils from Chile and includes a positive partial
206 slope for the CEC. The CEC value can be viewed as a proxy for the sum of clay and soil OM contents, so that the over whole
207 partial slope of OM is compensated in that particular situation.

Table 1.: Transfer functions reviewed from literature to estimate partition coefficient of Cu. R.V stands for response variable and Int. for intercept. Most studies fitted K_f defined as $K_f = [Cu]_{soil}/[Cu]_{solution}^{n-opt}$ in $L.kg^{-1}$, Cu_{soil} or Cu tot in $mg.kg^{-1}$, DOC (dissolved organic carbon) in $mg.L^{-1}$, OM (soil organic matter) in %, CEC in $cmol.kg^{-1}$, standard error around fitted coefficient are reported when indicated in the original article.

Author	Eq	R.V	Int.	Log (Cu tot)	pH	Log (OM)	Log (DOC)	other	n-opt	R2	number of data	Range Cu tot	Range OM	Range DOC	Range pH
(Vulkan et al., 2000)	4	Log (K_f)	1.74		0.34		-0.58		1	0.42	21	19-8645		9.8-69.8	5.5-8
(Sauvé et al., 2000)	5a	Log (K_f)	1.49 ±0.13		0.27 ±0.02				1	0.29	447	6.8-82850			
(Sauvé et al., 2000)	5b	Log (K_f)	1.75 ±0.12		0.21 ±0.02	0.51 ±0.06			1	0.42	353	6.8-82850			
(Degryse et al., 2009)	6a	Log (K_f)	0.6		0.37				1	0.34	129				
(Degryse et al., 2009)	6b	Log (K_f)	0.45		0.34			0.65 log (CEC %)	1	0.44	128				
(Unamuno et al., 2009)	7a	Log (K_f)	1.95		0.16				1	0.15	29	18-10389			
(Unamuno et al., 2009)	7b	Log (K_f)	2.383	0.46					1	0.61	29	18-10389			
(Unamuno et al., 2009)	7c	Log (K_f)	1.99	0.42	0.06				1	0.63	29	18-10389			
(Groenenberg et al., 2010)	8a	Log (K_f)	2.26		0.89	0.9			0.85	0.87	216	0.1-326	2-97.8		3.3-8.3
(Ivezić et al., 2012)	9a	Log (K_f)	3.98			0.48	-0.59		1	0.5	74	5.7-141		0.9-10.2	4.3-8.1
(Mondaca et	10a	Log	1.05	0.7		-1.06			1	0.46	86	56-	12.0-62		6.2-7.8

al., 2015)		(K_f)										4441			
(Mondaca et al., 2015)	10b	Log (K_f)	2.88	0.41			-1.03		1	0.77	86	56-4441	12.0-62		6.2-7.8
(Li et al., 2017)	11a	Log (K_f)	3.12	0.47			-0.66		1	0.28	34				
(Li et al., 2017)	11b	Log (K_f)	2.179	-0.45 * log (Cu solution) $\mu mol.L^{-1}$					1	0.42	34				
(Li et al., 2017)	11c	Log (K_f)	2.59	0.617			-1.55		1	0.88	20				

211

Over the 15 equations, the estimation of K_f according to (Sauvé et al., 2000) with Eq. (5a) or (5b) (Table 1) is the most robust as determined over a wide range of soils (more than 400 points). The estimations are based on a large gradient of in situ total soil Cu concentrations, even though the highest total soil Cu concentration is higher than what was observed in Europe with the JRC''s soil survey (Ballabio et al., 2018). Sauvé et al., (2000) proposed two equations based on a compilation of about 400 data points from long-term contaminated samples. One of the equations considers OM values, whereas the other does not due to a lack of information in the gathered data. Finally, due to the well-known importance in OM for binding with Cu, the Eq. (5b) was selected for our application at the Europe scale and K_f was calculated as following:

$$(K_f) = 1.75 + 0.21pH + 0.51(OM)$$

with K_f in $L.Kg^{-1}$ and OM being the soil organic matter content calculated as OM = 2 x OC from JRC following (Pribyl, 2010).

K_f values display a range of 4600 to 21500 $L.kg^{-1}$ with a median value of 9829 $L.kg^{-1}$. K_f values below 8000 $L.kg^{-1}$ and above 12000 $L.kg^{-1}$ respectively represent low and high anomalies for K_f. On the European scale, a heterogeneous distribution can be seen when using equation (5b), as shown in (Fig. 1).

Beyond the E''s administrative borders (*e.g.* Switzerland and Norway), in certain mountain areas there is a lack of OC data which is''t supplied by the JRC. Cu partitioning in soil solution is low around the Mediterranean, UK, Baltic and Nordic regions with high K_f (>12000 $L.kg^{-1}$). This accounts for 29.9 % of the grid cells, where deposited Cu can thus accumulate in soils. On the contrary, high partition of Cu into soil solution can be found in 20.1% of the grid cells where values of K_f are low (<8000 $L.kg^{-1}$), thus providing soils with a tendency to f copper for other ecosystems, depending on the runoff. This occurs for instance near Portugal and Poland.

3.2. Modelling potential Cu leaching and accumulation in European soils for the historical period (2001-2005)

Over the two LSMs x 2 GCMs, the runoff values during the 2001-2005 period varied between 0 (LPJmL_CM5a and LPJmL_ESM2m) and 5.4 $mm.day^{-1}$ (LPJmL_CM5a). The mean runoff value over the two LSMs x 2 GCMs is 1.1 (± 0.1 standard deviation) $mm.day^{-1}$ (data shown in Fig S1). For this period, the 1MAD threshold gives rather similar low and high runoff anomalies between couples of LSMs x GCMs, below 0.6, 0.6, 0.7, 0.6 $mm.day^{-1}$ and above 1.3, 1.2, 1.3 and 1.1 $mm.day^{-1}$ respectively for ORCHIDEE_CM5a, ORCHIDEE_ESM2m, LPJmL_CM5a and LPJmL_ESM2m. In addition, respectively 21.7, 22.1, 20.2 and 21.1 % of the grid cells are low runoff anomalies and 28.2, 27.9, 29.8 and 28.9 % of the grid cells are high runoff anomalies (see Table S1).

Fig. 2 represents the LP and AP areas for the 2001-2005 period and for the different combinations of LSMs and GCMs. The amount of grid cells with LP and AP areas varied among the LSMs x GCMs combinations (Fig. 3 with the historical scenario and Table S1). However, spatial patterns are well conserved with more similarities between the same LSM than

between the same GCM. Globally, LP areas are located mostly in Northern Portugal with scattered points around France, Germany and Scandinavia while AP areas are mostly found in South East of Spain, South-Adriatic coast of Italy and scattered points in Hungary. But, with the ORCHIDEE LSM, AP areas in South Spain are larger, and LP areas in France and East Europe are more scattered than with the LPJmL LSM.

Over the four combinations of LSMs and GCM, LP was detected in 6.4 ± 0.1 % (median, median deviation) of the grid cells are (Fig. 3 (a)) and AP was detected in 6.7 ± 1.1 % of the grid cells (Fig. 3(b)). Areas with LP are almost equal between all LSMs x GCMs even if ESM2m forcing leads to slightly less areas with LP than CM5a. Much more AP areas are predicted by ORCHIDEE LSM. LPJmL_CM5a combination has the smallest percentage of the grid cells with AP with 5.5 %, while ORCHIDEE_CM5A has the largest percentage with 8.0 % (Fig. 3(b)).

3.3. Modelling the changes of the LP areas over the century according to the different RCPs

For the two chosen climate change scenarios, median runoffs per models are expected to increase over the century for the 2 LSMs x 2 GCMs combinations. For the 2051-2055 period, predicted runoff is 1.1 ± 0.1 $mm.day^{-1}$ with RCP 2.6 and RCP 6.0 (mean, standard deviation of the 2 LSMs x 2 GCMs over the 5 years), (see Fig. S2 for RCP 2.6 and Fig. S4 for RCP 6.0). For the 2091-2095 period, predicted runoff is also 1.1 ± 0.1 $mm.day^{-1}$ with RCP 2.6 but 1.0 ± 0.1 $mm.day^{-1}$ with RCP 6.0 (mean, standard deviation of the 2 LSMs x 2 GCMs over the 5 years), (Fig. S3 for RCP 2.6 and Fig. S5 for RCP 6.0). Table S1 shows that the amount of grid cells defined as high anomalies for runoff tends to decrease by the 2091-2095 period while the amount of grid cells defined as low anomalies for runoff tends to increase. However, tendencies for the 2051-2055 period are variable with in some cases an increase or a decrease in percentage by comparison with the previous or subsequent periods (see Table S1). Furthermore, among the different periods of climate change scenarios, the ratio of LP areas in percentage over areas of high anomalies for runoff is not constant (see Table S1).

The changeof areas in Europe with LP for the different climate scenarios and the different LSMs x GCMs combinations over the century is presented in percentage in Fig. 3(a). Compared to the historical values and whatever the scenario, the median percentage of grid cells with LP in 2091-2095 decreases by 1.2 ± 0.3 percentage points (median, median deviation) for RCP 2.6 and by 2.1 ± 0.5 percentage points for RCP 6.0. Hence, for the 2091-2095 period, percentage of surfaces with LP are 5.3 ± 0.3 % (median, median deviation) for RCP 2.6 and 4.3 ± 0.6 % for RCP 6.0. Areas where LP was detected are relatively similar for all the time period and climate change scenarios and for all LSMs x GCMs except ORCHIDEE_ESM2m that always predicted the smallest percentage of areas with LP. Indeed, for ORCHIDEE_ESM2m the percentage of areas with LP are from 59% (RCP 6.0 2091-2095) to 79 % (RCP 6.0 2051-2055) smallest than the median percentage of surfaces with LP (see Fig. 3(a)).

The change of LP's median during the century depends on the climate change scenario. With RCP 2.6, the median percentage of grid cells with LP varied more between the historical scenario and the 2051-2055 one (-0.8 ± 0.4 percentage points, median,

median deviation) than between the 2051-2055 and the 2091-2095 periods (-0.4 ± 0.3 percentage points). On the contrary, with RCP 6.0, the median percentage of grid cells with LP areas decreases less from the historical scenario to the 2051-2055 one (-0.3 ± 0.2 percentage points, median, median deviation), than between the 2051-2055 and 2091-2095 periods (-2.0 ± 0.2 percentage points), see Fig. 3 (a). Furthermore, with RCP 2.6, estimations give 5.5 ± 0.5 % of the grid cells with LP in 2051-2055 and 6.2 ± 0.2% with RCP 6.0, which is similar to the 2001-2005 estimate.

For all LSMs and GCMs and the two RCPs, LP areas are mostly detected in Portugal, north Germany and Scandinavia. In terms of LP risks, the combinations of GCMs and climate change scenarios mostly affect the quantity of dispersed spots in East Europe and in the southern regions of Portugal. By 2050, the decrease in LP areas is mostly located in the center of France, south of Portugal and north of Germany (Fig. 4 for the RCP 2.6 and Fig. 6 for the RCP 6.0). By 2090, the decrease in LP areas are mostly located in the south of Portugal (Fig. 5 for the RCP 2.6 and Fig. 7 for the RCP 6.0)

3.4. Modelling the changes of the AP areas over the century according to the different RCPs

The change of AP areas in Europe w the different climate scenarios and the different LSMs x GCMs combination over the century is presented in percentage in Fig. 3(b). For the 2091-2095 period and for the two climate change scenarios, the percentage of grid cells an AP is detected increases for all LSMs x GCMs except for ORCHIDEE_CM5a with RCP 2.6. AP area increases are highly variable between LSMs x GCMs, with a smaller increase between historical period and 2091-2095 for RCP 2.6 than for RCP 6.0.

With RCP 2.6, and for all LSMs x GCMs, the percentage of grid cells where an with AP is detected increases between the historical scenario and the 2051-2055 period. Between 2051-2055 and 2091-2095, the percentage of grid cells where AP is detected increases for LSMs_ESM2m and decreases for LSMs_CM5a (see Fig. 3 (b)).

With RCP 6.0, the percentage of areas where AP is detected increases for all LSM x GCM except with ORCHIDEE_CM5a between the historical period and the 2051-2055 period, and for all LSM x GCM combinations between the 2051-2055and the 2091-2095 period.

For all LSMs X GCMs and the two RCPs, AP areas are found in Sicilia, East Europe and South Spain. However, the density and extent of the AP areas in these regions varied between LSMs x GCMs and climate change scenarios (Fig. 4 and 5 for the RCP 2.6 for the 2051-2055 and by 2091-2095 periods, respectively and Fig. 6 and 7 for the RCP 6.0 for the 20510-2055 and by 2091-2095 periods, respectively). Over the century, we found new AP areas in East Europe and Greece.

Finally, over all LSMs x GCMs and climate change scenarios, the extent of areas presenting LP and AP in each region rather depends on GCM than on LSM, with more similarities between ORCHIDEE_GCM (sub figures (a) and (b) in Fig. 2, 4, 5, 6, 7) and LPJmL_GCM (sub figures (c) and (d) in Figs. 2, 4, 5, 6, 7) than between LSM_CM5a (sub figures (a) and (c) in Figs. 2, 4, 5, 6, 7) and LSM_ESM2m (sub figures (b) and (d) in Figs. 2, 4, 5, 6, 7).

4. Discussion

4.1. Modelling soil copper release or storage with time for contaminated soils

This study aims at identifying potential leaching soil areas for Cu over Europe in order to identify locations where soil may play a role in the Cu transfer from soil to aquatic ecosystems. To estimate the proportion of Cu reaching soil solution, we chose to focus on the partitioning coefficient which was calculated based on soil properties (pH and OM here) other than total soil Cu. This specific choice of K_f coefficient rather than considering only the soil total Cu contents was made because Cu in solution is not strictly correlated with total Cu, nor with other single soil properties as for instance pH and soil OM which are both known to affect Cu partitioning and mobility. Thus, taking into account the variability of soil properties at the European scale, the spatial distribution of Cu in solution was shown to be different from the spatial distribution of total Cu (Sereni et al., 2022a). However, data on Cu in solution at large scales are not available making impossible the direct estimation of transport within soil solution and of AP or LP areas without using the K_f. Finally, the use of partition coefficient allowed us to estimate risk areas without considering total soil Cu temporal variability and with the hypothesis that pedological soil characteristics will not change at the time scale studied. This is a strong implicit assumption but needed at that stage. Indeed, even though some soil OM projections are available (Varney et al., 2022) to our knowledge, future projections of pH values at European scale due to climate change are not available limiting our capacities to calculate a time-dependent K_f. In particular, there are large uncertainties about the C stocks that may change as a result of climate change and dedicated policies for increasing the C stocks (Bruni et al., 2022). Besides, organic fertilizers applied to increase C stocks can change both pH and soil Cu content leading to supplementary uncertainties (Laurent et al., 2020). Furthermore, together with rainfall and soil moisture changes, climate change is expected to also induce higher temperatures and shorter winters, so that a shift in cultures toward the North is expected (Hannah et al., 2013). Therefore, areas with currently low total soil Cu levels may potentially experience a rise in Cu inputs from fungicides, which may subsequently be transported through freshwater systems. Thus, the estimations of LP and AP as computed here, can be used to identify regions about to leach or accumulate high amount of Cu and anticipate total content modifications that could occur with an eventual change in anthropogenic activities. Indeed, land management changes due to land use changes or regulation changes may affect the use of Cu in agriculture in the future with potential consequences on Cu leaching.

As a first step, the study conducted here could be used to highlight areas needing regulations to lower Cu input thresholds. Indeed, the changes of the LP (and AP) areas we noticed are not only the reflection of the general runoff change or of the current Cu risk but also underline areas of interest when combining risk linked to soil contamination and climate change. For instance, in Eastern Europe, low K_f and high runoff result in Cu LP areas with soils tending to transfer Cu from soils to the other ecosystems. However, in these cases, low amounts of total soil Cu contents (Ballabio et al., 2018) limit the amount of Cu exports. In parallel, in Italy, we found high AP areas whatever the LSMxGCM and RCP for at least one studied period and one RCP examined. In these vineyard regions (Abruzo, Marche regions), annual Cu inputs are high, resulting in Cu accumulation in soil surface horizons. These high total Cu concentrations could further enter the food web (García-Esparza et al., 2006) or be exported with soil particles (Imfeld et al., 2020) due to rain erosion (El Azzi et al., 2013). Highly erosive storm events predicted to increase during the next decades in Europe are another risk factor for freshwater contamination even in AP areas, but are often very punctual and local Hence, to go further on, localization of areas with exogenous risks of Cu dissemination have to be identified to reinforce the predictions, e.g. by coupling studies of leaching potential as the one we conducted here with erosion risk studies (Panagos et al., 2021)and with outlet characteristics.

351

352 4.2. Temporal change of data and scope of the modelling analysis

353 To reduce intra and inter annual variability the modelling conducted here focused on 5-years means, thus aimed at smoothing
354 seasonal variability of runoff. The K_f we calculated was not a dynamic value since we did not make hypothesis about the
355 temporal change of soil organic carbon or pH. Furthermore, K_f is defined on the assumption that there is equilibrium between
356 the solid and solution phases. This means that the amount of Cu in solution estimated by this method may be less than that
357 present immediately after Cu application and before equilibrium is reached (McBride et al., 1997). Nevertheless, our results
358 showed a good agreement between the four LSMs x GCMs in their projection of the number of grid cells where both LP and
359 AP are detected, validating the use of their median to perform projections in the absence of in situ validation.
360 It must be noted that the scope of our predictions had limits that rely on the difficulties to predict whether rain- and snow-falls
361 and runoff will evolve in terms of intensity and frequency . It has already been identified that during high loads events, much
362 more Cu was transported in solution than during light events (Imfeld et al., 2020) but alternations of drying and rewetting
363 events may also affect Cu partitioning between phases (Christensen and Christensen, 2003; Han et al., 2001). Also, to gain
364 field reality at the local scale (here, up to 50 km) such as landscape or catchment for example, modelling will require to account
365 for the time periods of year with higher rain- and snowfalls amounts coinciding with periods of Cu use, for instance in
366 agriculture and vineyards (Ribolzi et al., 2002; Banas et al., 2010). Indeed, if intense rainfall occurs close to Cu fungicide
367 applications, a larger Cu amount than locally computed taking into account total Cu and K_f may be exported through runoff
368 (Ma et al., 2006b, a). Thus, local soil Cu budgets require the use of temporal model, which accounts for the regular inputs and
369 outputs of Cu from vegetation and runoff that cannot be accounting with multiyear mean. Finally, the identification of the areas
370 with high risks of soil Cu leaching or accumulation we made in this study can be viewed as a first step for the risk change
371 assessment of Cu contamination useful for land management or Cu-fertilizer applications regulations.
372

373 5. Conclusion

374 Our approach to assess European areas with a potential to accumulate or leach copper from soils was not straightforward but
375 included several steps. We focused first on the methods to calculate Cu partitioning. By reviewing existing Cu K_f's equations
376 we pointed out pH and soil OM contents as important determinants and more precisely that the OM partial effect was larger
377 than the pH one. Then, using the European maps of soil characteristic data, we computed the map of K_f at the 0.5° scale,
378 highlighting areas with high risk to leach or to accumulate Cu for a given soil. The estimation of LP and AP areas for current
379 and future soil runoffs under two RCPs with couples of two GCMs x two LSMs was thereafter performed by comparing
380 anomalies for both K_f and runoffsWe hence provided a new method to emphasize at the regional scale the combined risk of
381 both climate change and contamination. We pointed out that despite similar projections for the end of the 21st century, the trend
382 during the century depends on the climate change scenario. For the historical period (2001-2005) our study showed comparable
383 amounts of grid cells where LP or AP is detected (between [6.2% - 6.4%] and between [5.5% - 8.0%], respectively). During
384 the century, AP areas were found to increase for all the LSMs x GCMs and the two RCPs. On the contrary, for the two RCPs
385 and three over the four LSMs x GCMs, LP areas were found to decrease during the century compared to the current estimation.
386 Surprisingly, the total number of grid cells where AP and LP are detected in 2091-2095 is r estimated between 13.2 ± 1.3 (RCP
387 2.6) and 14.6 ± 1.3% (RCP 6.0). This was due, however, to opposite trends in the change of LP areas that decrease and AP
388 areas that increase during the century. We highlighted the areas of particular risk for application of Cu, emphasizing the

necessity to precise monitoring in Cu application on these areas. Future studies would gained in precision by taking into account the change of partitioning coefficient with soil change or scenarios of Cu application taking into account the various forms (e.g., mineral or organic fungicides).

Figures captions:

Fig. 1: Map of $\log_{10}(K_f)$ in Europe at 0.5° following Eq. (5b) applied to soil Cu contents. White pixels correspond to pixel without OC measurement, and consequently no K_f estimations.

Fig. 2: Areas of potential for Cu leaching (LP) and accumulation (AP) over the historical (2001-2005) period for the combinations of land surface scheme (ORCHIDEE in (a), (b) ; LPJmL in (c), (d)) and climate forcing (CM5a in (a), (c) and ESM2m in (b), (d)). White pixels correspond to pixel without OC measurement, and consequently no Kf estimations.

Fig. 3: Percentage of the grid cells with Cu LP (a) and AP (b) for the different scenarios (historical=2001-2005, RCP 2.6 horizon 2050 and 2090 and RCP 6.0 horizon 2090). The 4 combinations of the 2 LSMs (ORCHIDEE in green and LPJmL in orange) and the 2 climate forcings (CM5a fill bars and ESM2m dashed bar) as well than median (purple) of the 4 models and median deviation (bar) are plotted.

Fig. 4: Areas of potential for Cu leaching (LP) and accumulation (AP) over the RCP2.6 2051-2055 period for the different combinations of land surface schemes (ORCHIDEE in (a), (b) ; LPJmL in (c), (d)) and climate forcings (CM5a in (a), (c) and ESM2m in (b), (d)). White pixels correspond to pixel without OC measurement, and consequently no Kf estimations.

Fig. 5: Areas of potential for Cu leaching (LP) and accumulation (AP) over the RCP 2.6 2091-2095 period for the different combinations of land surface schemes (ORCHIDEE in (a), (b) ; LPJmL in (c), (d)) and climate forcings (CM5a in (a), (c) and ESM2m in (b), (d)). White pixels correspond to pixel without OC measurement, and consequently no Kf estimations..

Fig. 6: Area of potential of leaching (LP) and accumulation (AP) over the RCP 6.0 2051-2055 period for the different combination of land surface scheme (ORCHIDEE in (a), (b) ; LPJmL in (c), (d)) and climate forcings (CM5a in (a), (c) and ESM2m in (b), (d)). White pixels correspond to pixel without OC measurement, and consequently no Kf estimations.

Fig. 7: Areas of Cu potential for leaching (LP) and accumulation (AP) potential over the RCP 6.0 2091-2095 period for the

different combinations of land surface schemes (ORCHIDEE in (a), (b) ; LPJmL in (c), (d)) and climate forcings (CM5a in (a), (c) and ESM2m in (b), (d)). White pixels correspond to pixel without OC measurement, and consequently no K_f estimations.

Code availability:

The code can be provided upon request.

Data availability:

The data can be provided upon request. Soil data are available on the ESDAC (Panagos et al., 2022; ESDAC - European Commission, 2024, 2012) and runoff data on ISIMIP (The Inter-Sectoral Impact Model Intercomparison Project, 2021)

Credit authorships contribution statement:

Laura Sereni: Methodology, Formal analysis, Data processing, Writing original draft.

Julie-Mai Paris: Formal analysis, Initial data processing, Writing original draft.

Isabelle Lamy: Methodology Conceptualization, Writing review and editing, Supervision, Funding acquisition

Bertrand Guenet: Methodology, conceptualization, Writing review and editing, supervision, Project administration,

Declaration of competing interests

The authors declare that they have no known competing financial interests or personal relationships that could have appeared to influence the work reported in this paper.

Acknowledgments

Parts of this study were financially supported by the Labex BASC through the Connexion project. LS thanks the Ecole Normale Supérieure (ENS) for funding her PhD. The authors thank Nathalie de Noblet-Ducoudré for valuable discussions on this paper.

Bibliography:

Babcsányi, I., Chabaux, F., Granet, M., Meite, F., Payraudeau, S., Duplay, J., and Imfeld, G.: Copper in soil fractions and

runoff in a vineyard catchment: Insights from copper stable isotopes, Science of the Total Environment, 557–558, 154–162, https://doi.org/10.1016/j.scitotenv.2016.03.037, 2016.

Ballabio, C., Panagos, P., and Monatanarella, L.: Mapping topsoil physical properties at European scale using the LUCAS database, Geoderma, https://doi.org/10.1016/j.geoderma.2015.07.006, 2016.

Ballabio, C., Panagos, P., Lugato, E., Huang, J. H., Orgiazzi, A., Jones, A., Fernández-Ugalde, O., Borrelli, P., and Montanarella, L.: Copper distribution in European topsoils: An assessment based on LUCAS soil survey, Science of the Total Environment, 636, 282–298, https://doi.org/10.1016/j.scitotenv.2018.04.268, 2018.

Banas, D., Marin, B., Skraber, S., Chopin, E. I. B., and Zanella, A.: Copper mobilization affected by weather conditions in a stormwater detention system receiving runoff waters from vineyard soils (Champagne, France), Environmental Pollution, 158, 476–482, https://doi.org/10.1016/j.envpol.2009.08.034, 2010.

de Brogniez, D., Ballabio, C., Stevens, A., Jones, R. J. A., Montanarella, L., and van Wesemael, B.: A map of the topsoil organic carbon content of Europe generated by a generalized additive model, European Journal of Soil Science, https://doi.org/10.1111/ejss.12193, 2015.

Broos, K., Warne, M. S. J., Heemsbergen, D. A., Stevens, D., Barnes, M. B., Correll, R. L., and McLaughlin, M. J.: Soil factors controlling the toxicity of copper and zinc to microbial processes in Australian soils, Environmental Toxicology and Chemistry, https://doi.org/10.1897/06-302R.1, 2007.

Bruni, E., Chenu, C., Abramoff, R. Z., Baldoni, G., Barkusky, D., Clivot, H., Huang, Y., Kätterer, T., Pikuła, D., Spiegel, H., Virto, I., and Guenet, B.: Multi-modelling predictions show high uncertainty of required carbon input changes to reach a 4‰ target, European J Soil Science, 73, e13330, https://doi.org/10.1111/ejss.13330, 2022.

Christensen, J. H. and Christensen, O. B.: Severe summertime flooding in Europe, Nature, 421, 805–806, https://doi.org/10.1038/421805a, 2003.

Chu, H., Wei, J., Qiu, J., Li, Q., and Wang, G.: Identification of the impact of climate change and human activities on rainfall-runoff relationship variation in the Three-River Headwaters region, Ecological Indicators, 106, https://doi.org/10.1016/j.ecolind.2019.105516, 2019.

Degryse, F., Smolders, E., and Parker, D. R.: Partitioning of metals (Cd, Co, Cu, Ni, Pb, Zn) in soils: concepts, methodologies, prediction and applications – a review, European Journal of Soil Science, 60, 590–612, https://doi.org/10.1111/j.1365-2389.2009.01142.x, 2009.

Douville, H., Raghavan, K., Renwick, J., Allan, R. P., Arias, P. A., Barlow, M., Cerezo-Mota, R., Cherchi, T., Gan, A. Y., Gergis, J., Jiang, D., Khan, A., Pokam Mba, W., Rosenfeld, D., Tierney, J., and Zolina, O.: Climate Change 2021: The Physical Science Basis. Contribution of Working Group I to the Sixth Assessment Report of the Intergovernmental Panel on Climate Change, in: Fundamental and Applied Climatology, vol. 2, edited by: Masson-Delmotte, V., Zhai, P., Pirani, A., Connors, S.

L., Péan, C., Berger, S., Caud, N., Chen, Y., Goldfarb, L., Gomis, M. I., Huang, M., Leitzell, K., Lonnoy, E., Matthews, J. B. R., Maycock, T. K., Waterfield, T., Yelekçi, O., Yu, R., and Zhou, B., cambride universitary press, 13–25, https://doi.org/10.21513/2410-8758-2017-2-13-25, 2021.

Dufresne, J. L., Foujols, M. A., Denvil, S., Caubel, A., Marti, O., Aumont, O., Balkanski, Y., Bekki, S., Bellenger, H., Benshila, R., Bony, S., Bopp, L., Braconnot, P., Brockmann, P., Cadule, P., Cheruy, F., Codron, F., Cozic, A., Cugnet, D., de Noblet, N., Duvel, J. P., Ethé, C., Fairhead, L., Fichefet, T., Flavoni, S., Friedlingstein, P., Grandpeix, J. Y., Guez, L., Guilyardi, E., Hauglustaine, D., Hourdin, F., Idelkadi, A., Ghattas, J., Joussaume, S., Kageyama, M., Krinner, G., Labetoulle, S., Lahellec, A., Lefebvre, M. P., Lefevre, F., Levy, C., Li, Z. X., Lloyd, J., Lott, F., Madec, G., Mancip, M., Marchand, M., Masson, S., Meurdesoif, Y., Mignot, J., Musat, I., Parouty, S., Polcher, J., Rio, C., Schulz, M., Swingedouw, D., Szopa, S., Talandier, C., Terray, P., Viovy, N., and Vuichard, N.: Climate change projections using the IPSL-CM5 Earth System Model: From CMIP3 to CMIP5, Climate Dynamics, https://doi.org/10.1007/s00382-012-1636-1, 2013.

Dunne, J. P., John, J. G., Adcroft, A. J., Griffies, S. M., Hallberg, R. W., Shevliakova, E., Stouffer, R. J., Cooke, W., Dunne, K. A., Harrison, M. J., Krasting, J. P., Malyshev, S. L., Milly, P. C. D., Phillipps, P. J., Sentman, L. T., Samuels, B. L., Spelman, M. J., Winton, M., Wittenberg, A. T., and Zadeh, N.: GFDL's ESM2 global coupled climate-carbon earth system models. Part I: Physical formulation and baseline simulation characteristics, Journal of Climate, https://doi.org/10.1175/JCLI-D-11-00560.1, 2012.

El Azzi, D., Viers, J., Guiresse, M., Probst, A., Aubert, D., Caparros, J., Charles, F., Guizien, K., and Probst, J. L.: Origin and fate of copper in a small Mediterranean vineyard catchment: New insights from combined chemical extraction and δ65Cu isotopic composition, Science of the Total Environment, 463–464, 91–101, https://doi.org/10.1016/j.scitotenv.2013.05.058, 2013.

Elzinga, E. J., Van Grinsven, J. J. M., and Swartjes, F. A.: General purpose Freundlich isotherms for cadmium, copper and zinc in soils, European Journal of Soil Science, 50, 139–149, https://doi.org/10.1046/j.1365-2389.1999.00220.x, 1999.

ESDAC - European Commission: https://esdac.jrc.ec.europa.eu/, last access: 1 June 2024.

Flemming, C. A. and Trevors, J. T.: Copper toxicity and chemistry in the environment: a review, Water, Air, and Soil Pollution, 44, 143–158, https://doi.org/10.1007/BF00228784, 1989.

Frieler, K., Lange, S., Piontek, F., Reyer, C. P. O., Schewe, J., Warszawski, L., Zhao, F., Chini, L., Denvil, S., Emanuel, K., Geiger, T., Halladay, K., Hurtt, G., Mengel, M., Murakami, D., Ostberg, S., Popp, A., Riva, R., Stevanovic, M., SuzGBRi, T., Volkholz, J., Burke, E., Ciais, P., Ebi, K., Eddy, T. D., Elliott, J., Galbraith, E., Gosling, S. N., Hattermann, F., Hickler, T., Hinkel, J., Hof, C., Huber, V., Jägermeyr, J., Krysanova, V., Marcé, R., Müller Schmied, H., Mouratiadou, I., Pierson, D., Tittensor, D. P., Vautard, R., Van Vliet, M., Biber, M. F., Betts, R. A., Leon Bodirsky, B., Deryng, D., Frolking, S., Jones, C. D., Lotze, H. K., Lotze-Campen, H., Sahajpal, R., Thonicke, K., Tian, H., and Yamagata, Y.: Assessing the impacts of 1.5°C global warming - Simulation protocol of the Inter-Sectoral Impact Model Intercomparison Project (ISIMIP2b), Geoscientific Model Development, 10, 4321–4345, https://doi.org/10.5194/gmd-10-4321-2017, 2017.

García-Esparza, M. A., Capri, E., Pirzadeh, P., and Trevisan, M.: Copper content of grape and wine from Italian farms, Food

Additives and Contaminants, 23, 274–280, https://doi.org/10.1080/02652030500429117, 2006.

Giller, K. E., Witter, E., and Mcgrath, S. P.: Toxicity of heavy metals to microorganisms and microbial processes in agricultural soils: A review, Soil Biology and Biochemistry, 30, 1389–1414, https://doi.org/10.1016/S0038-0717(97)00270-8, 1998.

Goldewijk, K. K., Beusen, A., Doelman, J., and Stehfest, E.: Anthropogenic land use estimates for the Holocene - HYDE 3.2, Earth System Science Data, 9, 927–953, https://doi.org/10.5194/essd-9-927-2017, 2017.

Groenenberg, J. E., Römkens, P. F. A. M., Comans, R. N. J., Luster, J., Pampura, T., Shotbolt, L., Tipping, E., and De Vries, W.: Transfer functions for solid-solution partitioning of cadmium, copper, nickel, lead and zinc in soils: Derivation of relationships for free metal ion activities and validation with independent data, European Journal of Soil Science, 61, 58–73, https://doi.org/10.1111/j.1365-2389.2009.01201.x, 2010.

Han, F. X., Banin, A., and Triplett, G. B.: Redistribution of heavy metals in arid-zone soils under a wetting-drying cycle soil moisture regime, Soil Science, 166, 18–28, https://doi.org/10.1097/00010694-200101000-00005, 2001.

Hannah, L., Roehrdanz, P. R., Ikegami, M., Shepard, A. V., Shaw, M. R., Tabor, G., Zhi, L., Marquet, P. A., and Hijmans, R. J.: Climate change, wine, and conservation, Proceedings of the National Academy of Sciences of the United States of America, 110, 6907–6912, https://doi.org/10.1073/pnas.1210127110, 2013.

The Inter-Sectoral Impact Model Intercomparison Project: https://www.isimip.org/, last access: 28 May 2021.

Imfeld, G., Meite, F., Wiegert, C., Guyot, B., Masbou, J., and Payraudeau, S.: Do rainfall characteristics affect the export of copper, zinc and synthetic pesticides in surface runoff from headwater catchments?, Science of the Total Environment, 741, 140437, https://doi.org/10.1016/j.scitotenv.2020.140437, 2020.

Ivezić, V., Almås, Å. R., and Singh, B. R.: Predicting the solubility of Cd, Cu, Pb and Zn in uncontaminated Croatian soils under different land uses by applying established regression models, Geoderma, 170, 89–95, https://doi.org/10.1016/j.geoderma.2011.11.024, 2012.

Komárek, M., Čadková, E., Chrastný, V., Bordas, F., and Bollinger, J. C.: Contamination of vineyard soils with fungicides: A review of environmental and toxicological aspects, Environment International, 36, 138–151, https://doi.org/10.1016/j.envint.2009.10.005, 2010.

Krinner, G., Viovy, N., de Noblet-Ducoudré, N., Ogée, J., Polcher, J., Friedlingstein, P., Ciais, P., Sitch, S., and Prentice, I. C.: A dynamic global vegetation model for studies of the coupled atmosphere-biosphere system, Global Biogeochemical Cycles, https://doi.org/10.1029/2003GB002199, 2005.

Lange, S.: EartH2Observe, WFDEI and ERA-Interim data Merged and Bias-corrected for ISIMIP (EWEMBI), GFZ Data Services, 2016.

Laurent, C., Bravin, M. N., Crouzet, O., Pelosi, C., Tillard, E., Lecomte, P., and Lamy, I.: Increased soil pH and dissolved organic matter after a decade of organic fertilizer application mitigates copper and zinc availability despite contamination,

548 Science of the Total Environment, https://doi.org/10.1016/j.scitotenv.2019.135927, 2020.

549 Li, B., Ma, Y., and Yang, J.: Is the computed speciation of copper in a wide range of Chinese soils reliable?, Chemical
550 Speciation and Bioavailability, 29, 205–215, https://doi.org/10.1080/09542299.2017.1404437, 2017.

551 Ma, Y., Lombi, E., Oliver, I. W., Nolan, A. L., and McLaughlin, M. J.: Long-term aging of copper added to soils,
552 Environmental Science and Technology, 40, 6310–6317, https://doi.org/10.1021/es060306r, 2006a.

553 Ma, Y., Lombi, E., Nolan, A. L., and McLaughlin, M. J.: Short-term natural attenuation of copper in soils: Effects of time,
554 temperature, and soil characteristics, Environmental Toxicology and Chemistry, 25, 652–658, https://doi.org/10.1897/04-
555 601R.1, 2006b.

556 McBride, M., Sauvé, S., and Hendershot, W.: Solubility control of Cu, Zn, Cd and Pb in contaminated soils, European Journal
557 of Soil Science, 48, 337–346, https://doi.org/10.1111/j.1365-2389.1997.tb00554.x, 1997.

558 Mimikou, M. A., Baltas, E., Varanou, E., and Pantazis, K.: Regional impacts of climate change on water resources quantity and
559 quality indicators, Journal of Hydrology, 234, 95–109, https://doi.org/10.1016/S0022-1694(00)00244-4, 2000.

560 Mondaca, P., Neaman, A., Sauvé, S., Salgado, E., and Bravo, M.: Solubility, partitioning, and activity of copper-contaminated
561 soils in a semiarid region, Journal of Plant Nutrition and Soil Science, 178, 452–459, https://doi.org/10.1002/jpln.201400349,
562 2015.

563 Noll, M. R.: Trace Elements in Terrestrial Environments, 374–374 pp., https://doi.org/10.2134/jeq2002.3740, 2003.

564 Panagos, P., Van Liedekerke, M., Jones, A., and Montanarella, L.: European Soil Data Centre: Response to European policy
565 support and public data requirements, Land Use Policy, 29, 329–338, https://doi.org/10.1016/j.landusepol.2011.07.003, 2012.

566

567 Panagos, P., Ballabio, C., Himics, M., Scarpa, S., Matthews, F., Bogonos, M., Poesen, J., and Borrelli, P.: Projections of soil
568 loss by water erosion in Europe by 2050, Environmental Science and Policy, 124, 380–392,
569 https://doi.org/10.1016/j.envsci.2021.07.012, 2021.

570 Panagos, P., Van Liedekerke, M., Borrelli, P., Köninger, J., Ballabio, C., Orgiazzi, A., Lugato, E., Liakos, L., Hervas, J., Jones,
571 A., and Montanarella, L.: European Soil Data Centre 2.0: Soil data and knowledge in support of the EU, European J Soil
572 Science, 73, e13315, https://doi.org/10.1111/ejss.13315, 2022.

573

574 Pribyl, D. W.: A critical review of the conventional SOC to SOM conversion factor, Geoderma, 156, 75–83,
575 https://doi.org/10.1016/j.geoderma.2010.02.003, 2010.

576 R Core Team: R core team (2021), R: A language and environment for statistical computing. R Foundation for Statistical
577 Computing, Vienna, Austria. URL http://www. R-project. org, ISBN 3-900051-07-0, URL http://www.R-project.org/., 2021.

578 Ribolzi, O., Valles, V., Gomez, L., and Voltz, M.: Speciation and origin of particulate copper in runoff water from a
579 Mediterranean vineyard catchment, Environmental Pollution, 117, 261–271, https://doi.org/10.1016/S0269-7491(01)00274-3,

2002.

Rooney, C. P., Zhao, F. J., and McGrath, S. P.: Soil factors controlling the expression of copper toxicity to plants in a wide range of European soils, Environmental Toxicology and Chemistry, 25, 726–732, https://doi.org/10.1897/04-602R.1, 2006.

Salminen, R. and Gregorauskiene, V.: Considerations regarding the definition of a geochemical baseline of elements in the surficial materials in areas differing in basic geology, Applied Geochemistry, https://doi.org/10.1016/S0883-2927(99)00077-3, 2000.

Sauvé, S., Hendershot, W., and Herbert E., A.: Solid-Solution Partitioning of Metals in Contaminated Soils: Dependence on pH, Total Metal Burden, and Organic Matter, American Chemical Society, 1125–1131, https://doi.org/10.1021/es9907764, 2000.

Schulzweida, U.: CDO User Guide, , https://doi.org/10.5281/zenodo.2558193, 2019.

Sereni, L., Guenet, B., and Lamy, I.: Mapping risks associated with soil copper contamination using availability and bio-availability proxies at the European scale, Environmental Science and Pollution Research, https://doi.org/10.1007/s11356-022-23046-0, 2022a.

Sitch, S., Smith, B., Prentice, I. C., Arneth, A., Bondeau, A., Cramer, W., Kaplan, J. O., Levis, S., Lucht, W., Sykes, M. T., Thonicke, K., and Venevsky, S.: Evaluation of ecosystem dynamics, plant geography and terrestrial carbon cycling in the LPJ dynamic global vegetation model, Global Change Biology, https://doi.org/10.1046/j.1365-2486.2003.00569.x, 2003.

Unamuno, V. I. R., Meers, E., Du Laing, G., and Tack, F. M. G.: Effect of physicochemical soil characteristics on copper and lead solubility in polluted and unpolluted soils, Soil Science, 174, 601–610, https://doi.org/10.1097/SS.0b013e3181bf2f52, 2009.

Varney, R. M., Chadburn, S. E., Burke, E. J., and Cox, P. M.: Evaluation of soil carbon simulation in CMIP6 Earth system models, Biogeosciences, https://doi.org/10.5194/bg-19-4671-2022, 2022.

Vidal, M., Santos, M. J., Abrão, T., Rodríguez, J., and Rigol, A.: Modeling competitive metal sorption in a mineral soil, Geoderma, 149, 189–198, https://doi.org/10.1016/j.geoderma.2008.11.040, 2009.

Vulkan, R., Zhao, F. J., Barbosa-Jefferson, V., Preston, S., Paton, G. I., Tipping, E., and McGrath, S. P.: Copper speciation and impacts on bacterial biosensors in the pore water of copper-contaminated soils, Environmental Science and Technology, 34, 5115–5121, https://doi.org/10.1021/es0000910, 2000.

van Vuuren, D. P., Edmonds, J., Kainuma, M., Riahi, K., Thomson, A., Hibbard, K., Hurtt, G. C., Kram, T., Krey, V., Lamarque, J. F., Masui, T., Meinshausen, M., Nakicenovic, N., Smith, S. J., and Rose, S. K.: The representative concentration pathways: An overview, Climatic Change, 109, 5–31, https://doi.org/10.1007/s10584-011-0148-z, 2011.

West, T. S. and Coombs, T. L.: Soil as the Source of Trace Elements [and Discussion], Philosophical Transactions of the Royal Society of London. Series B, Biological Sciences, 294, 19–39, 1981.